

Original Research Article

Electrical and Morphological Properties of ion beams intermixed Zirconium/Silicon interface

V.Sisodia

Materials Science Lab, Department of Physics, Central University of Rajasthan, India.

Corresponding Author: V. Sisodia, Materials Science Lab, Department of Physics, Central University of Rajasthan, India.

Abstract

Zirconium (~ 60 nm) thin layer was deposited on Si (100) substrates in ultra high vacuum conditions using the electron-beam evaporation technique. The system was exposed to different ion fluencies ranging from 3×10^{13} – 1×10^{14} ions/cm² at room temperature. Zirconium silicide was synthesized on Si (100)/ zirconium interface by means of swiftly moving 150 MeV Au ion beam available from Tandem Accelerator in IUAC, India. Synthesized zirconium silicide thin film reasonably affects the resistivity of the irradiated system and for highest fluence of 1×10^{14} ions/cm² resistivity value reduces from 84.3 $\mu\Omega$.cm to 36 $\mu\Omega$.cm. A low resistivity silicide phase, C-49 ZrSi₂ was confirmed by X-ray analysis. Schottky barrier height was calculated from I-V measurements and the values drops down to 0.58 eV after irradiation at 1×10^{14} ions/cm². The surface and interface morphologies of zirconium silicide were examined by atomic force microscopy (AFM) and scanning electron microscopy (SEM). AFM shows a considerable change in the surface structure and SEM shows the ZrSi₂ agglomeration and formation of Si-rich silicide islands.

Keywords: swift heavy ion, irradiation, ion beam

Introduction

Integrated circuit manufacturing today is dominated by transition metal silicides; these are typically employed as low resistance contacts to metal–oxide–semiconductor field effect transistors. The field is rich with many novel methods for refining the manufacturing processes and improving performance. From some time, the effects of ion-beam mixing on the growth of silicides have been explored (Xia et al., 1989; Hamdi and Nicolet, 1984; Niewoñner and Depta, 1991; Ye et al., 1991; Dehm et al., 1993; Kasko et al., 1993; Baba et al., 1997; Kal et al., 1995; Hung et al., 1989; Wielunski et al., 1982).

Metal silicides such as MoSi₂ and TiSi₂ are of interest as interconnections and contacts in sub-100 nm gate MOSFET devices (Murarka, 1980; Murarka and Fraser, 1980; d’Heurle and Mater, 1998; Jeon et al., 1992; Maex and Mater, 1992). However, MoSi₂ has a high electric resistivity. Although TiSi₂ exhibits a quite low resistivity in the C54 phase (face-centered orthorhombic), it suffers from having a metastable low-temperature phase with four times higher resistivity. The metastable phase of TiSi₂ has an orthorhombic base-centered lattice structure, i.e. ZrSi₂ structure (C49), and the phase transition occurs at around 650°C (Jeon et al., 1992). Since zirconium is in the

Table 1: The Calculated structural parameters of Zr/Si thin films irradiated at fluences 6×10^{13} and 1×10^{14} ions/cm²

Fluence (ions/cm ²)	2θ	$d(\text{\AA})$	hkl	$D(\text{\AA})$	$\epsilon \times 10^{-3}$	$\delta \times 10^{15}$	
					(lin ² /m ⁻⁴)	(lin/m ²)	
ZrSi ₂	6×10^{13}	34.712	2.027	111	73.50	4.710	18.510
1×10^{14}	34.434	2.601	111	67.14	5.160	22.183	
ZrSi ₂	3×10^{13}	44.695	2.027	061	148.62	2.331	4.527
6×10^{13}	44.572	2.029	061	133.81	2.589	5.584	
1×10^{14}	44.572	2.030	061	113.64	3.049	7.743	
ZrSi ₂	6×10^{13}	64.538	1.442	152	67.70	5.114	21.818
1×10^{14}	64.786	1.437	152	67.45	5.118	21.980	
ZrSi ₂	6×10^{13}	77.612	1.228	242	74.69	4.638	17.925
1×10^{14}	77.736	1.227	242	62.54	5.397	25.567	

Table 2: The observed resistivity value and calculated Schottky barrier height of unirradiated and irradiated thin films

Irradiation dose (ions/cm ²)	resistivity ($\mu\Omega$.cm)	schottky barrier height (eV)
Unirradiated	210	0.62
3×10^{13}	84.3	0.61
6×10^{13}	41.2	0.61
1×10^{14}	36	0.58

same group (IVa) in the periodic table as Ti, Zr silicide is expected to have similar physical and chemical characteristics as Ti silicide. The Zr silicide formed by the thin film reaction with Zr deposited on silicon also exhibits a relatively low resistivity (35–40 $\mu\Omega$.cm) and high thermal stability (Sukow and Nemanich, 1994; Jeon et al., 1998)

A Schottky barrier height of 0.55 eV, about half of the Si band gap, was reported for ZrSi₂ on n-type Si (Lau et al., 1974). In addition, one advantage of ZrSi₂ over TiSi₂ is that it is stable in the C49 phase [Setton and Spiegel, 1991; Lin et al., 1996]. Structurally, ZrSi₂ has a peculiar pseudo lamellar crystal structure with lattice

parameters of $a = 0.369$ nm, $b = 1.47$ nm, and $c = 0.366$ nm (Bourret et al., 1990).

In addition, Zr oxide is a promising high-k dielectric material (Zhao et al., 2005), making ZrSi₂ highly compatible. The process employed is a technique of forming nanometer-scale zirconium silicide structures using IB (Ion beam) irradiation. The process relies on the effects of ion-beam mixing and radiation-induced diffusion, which together are instrumental in activating the sollicitation process across an interfacial boundary.

Much of this work has focused on the characterization of the role of irradiation on the formation of silicide phases.

In this paper, we report on our experimental investigations of Zr silicide nanostructural

growth on Si (100) surfaces using 150 MeV Au ion irradiation in terms of its structure, morphology, electrical properties and the phenomenon behind the electronic energy deposition mechanism.

The surface morphology of ZrSi₂ structure was studied using Scanning Electron microscopy (SEM) and Atomic force Microscopy (AFM).

Materials and methods

Thin film deposition and ion irradiation

Thin film samples used in the current experiment were deposited on Si (100) single crystals (n-type, 35Ω·cm) wafer using electron beam evaporator under UHV conditions at a base pressure of 1.5×10^{-8} torr. They were degreased by successively boiling in carbon tetrachloride, acetone and ethanol, and rinsed in deionized water. Then the samples were introduced into the UHV chamber. An amorphous layer of approximately 120 nm Si was deposited on the substrate to avoid the interference of native silicon oxide layer during ion beam mixing. A layer of approximately 60 nm thick Zr was then deposited on this Si layer. Finally, Si protective layer (30 nm) was deposited to avoid the oxidation of Zr layer. a-Si/Zr/a-Si samples were irradiated by 150 MeV Au⁺ ions using 15 UD Pelletron accelerator at IUAC, New Delhi, India for fluences in the range of 3×10^{13} – 1×10^{14} ions/cm² at room temperature. The samples were irradiated uniformly over an area of 1 cm × 1 cm by scanning the ion beam with a current ~1 pA, using an electromagnetic scanner. The vacuum in the irradiation chamber was low 10^{-6} torr. Ion range and deposited energy were calculated using SRIM software, (Zeigler et al., 1985) according to which the values of electronic and nuclear energy loss of 150 MeV Au ions in Zr are 26.73 keV/nm and 0.37 keV/nm and in Si are 14.43 keV/nm and 0.17 keV/nm respectively, signifying that the energy loss process by electronic excitation is prevailing over the nuclear reaction. It can

be suggested that mixing occurs at the interface of Zr/Si system, envisaged due to electronic energy deposition

Experimental Results and Discussion

Physical phase analysis by GIXRD

Grazing incidence X-ray diffraction was performed on unirradiated and irradiated samples in 2θ ranging from 20–90°. The XRD measurement instrument was Siemens Diffractometer D5000. X-ray beam was taken at a grazing angle of 0.5° to make the beam at most parallel with thin film, to stop the irradiation into substrate. Diffraction patterns were analyzed by using the PCPDFWIN program. Diffraction patterns of as-deposited and irradiated samples are shown in Fig.1. The unirradiated sample shows only metal peaks that correspond to (100), (200) and (202) planes of zirconium. After irradiation of the sample at fluence 3×10^{13} ions/cm², the intensity of Zr decreases, and this points to a slight diffusion of Zr in Si. Again for a higher irradiation fluence of 6×10^{13} ions/cm², four diffraction peaks of ZrSi₂ appears and planes are indexed as (111), (061), (152) and (242). Further on increasing ion fluence up to 1×10^{14} ions/cm², the height of ZrSi₂ peaks increases, suggesting the formation of well-crystallized ZrSi₂ phase of good quality. Initially, say for the fluence of 3×10^{13} ions/cm², as the ion beam passes through Zr thin film on Si, ZrSi₂ formation is promoted by ion irradiation, though the crystallinity of the formed phase was not good under that condition. Increasing the irradiation fluence to 1×10^{14} ions/cm² causes more atomic dislocations at the interface, enabling one to grow good quality ZrSi₂ which is shown in the XRD patterns of Fig.1. Diffractogram and X-ray analysis provides evidence for the formation of C-49 ZrSi₂ phase with different planes at the interface.

The calculated values for different ion fluencies are given in Table 1. Crystallite size (D) is calculated using the Scherrer formula from full width at half maximum

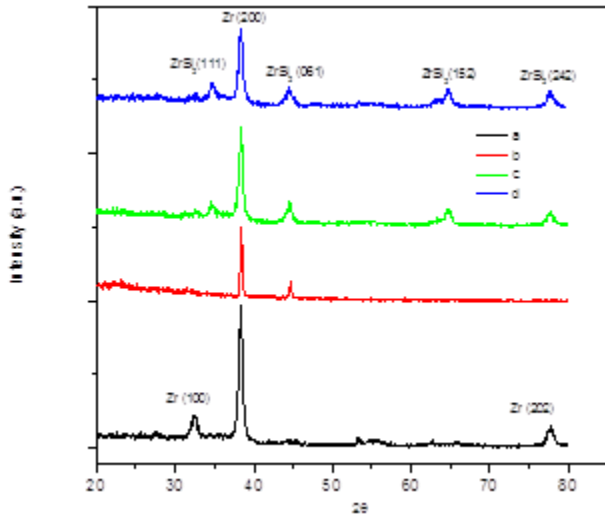
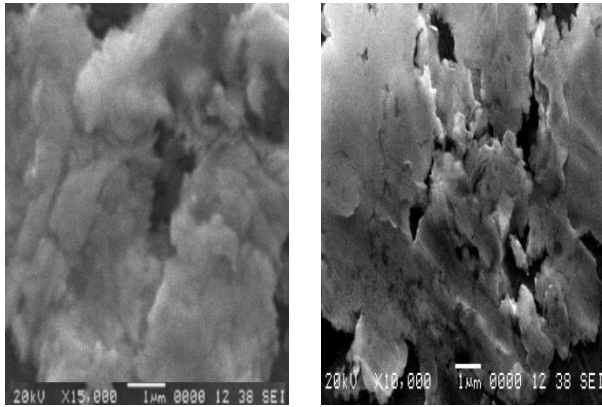


Figure 1: XRD spectra of the Zr–Si silicide films as a function of the irradiation doses, (a) virgin, (b) 3×10^{14} , (c) 6×10^{14} and (d) 1×10^{14} ions/cm².

(a) (b)



(c) (d)

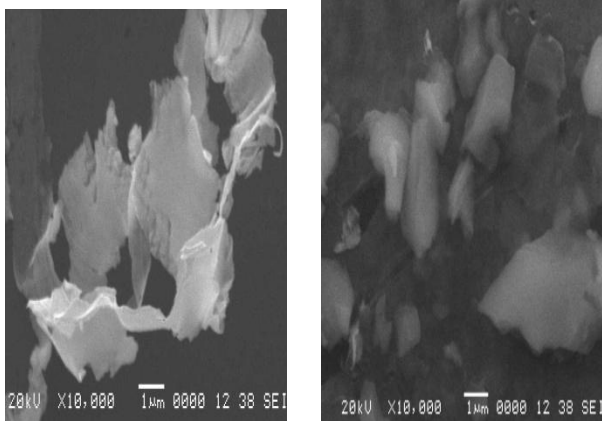
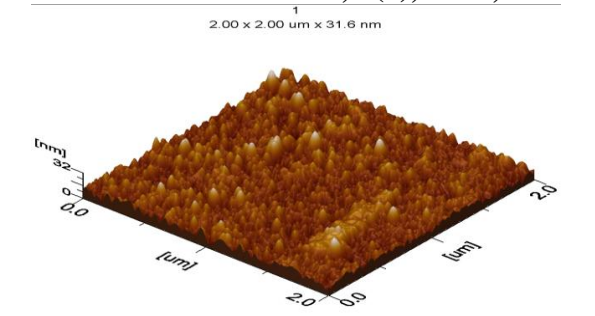
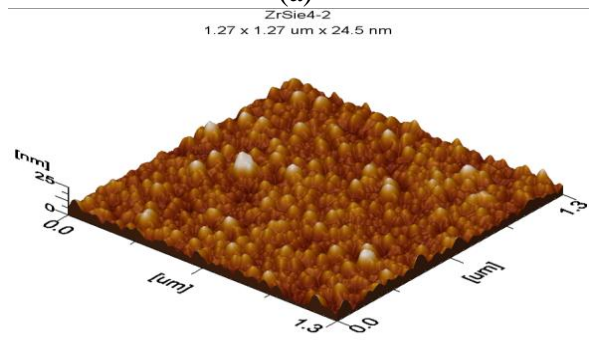


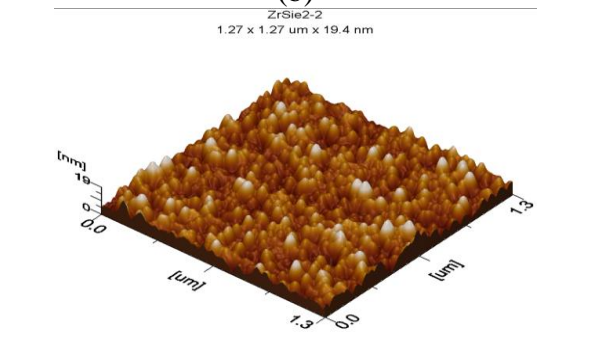
Figure 2: SEM micrographs of Zr–Si silicide films formed by ion irradiation at fluence: (a) no ions (b) 3×10^{13} ions/cm², (c) 6×10^{13} ions/cm² and (d) 1×10^{14} ions/cm².



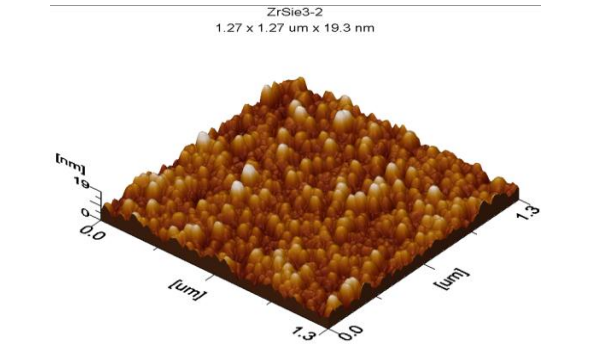
(a)



(b)



(c)



(d)

Figure 3: AFM images of the Zr–Si silicide films formed by ion irradiation at fluence: (a) no ions (b) 3×10^{13} ions/cm², (c) 6×10^{13} ions/cm² and (d) 1×10^{14} ions/cm².

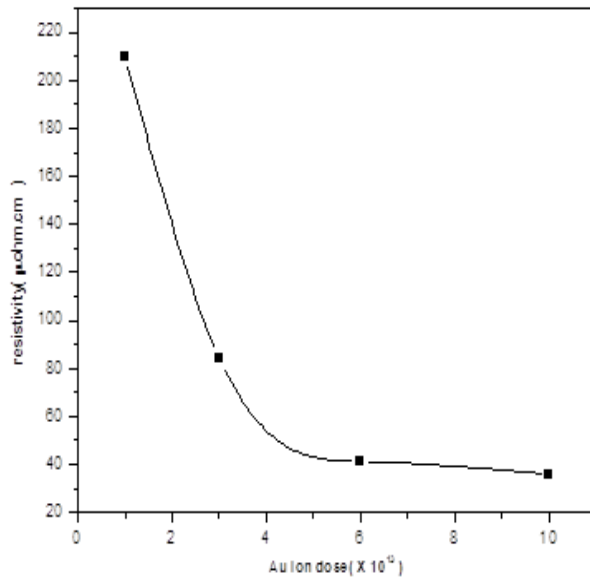


Figure 4: The variation of the resistivity of the Zr-Si silicide films as a function of the irradiation ion dose.

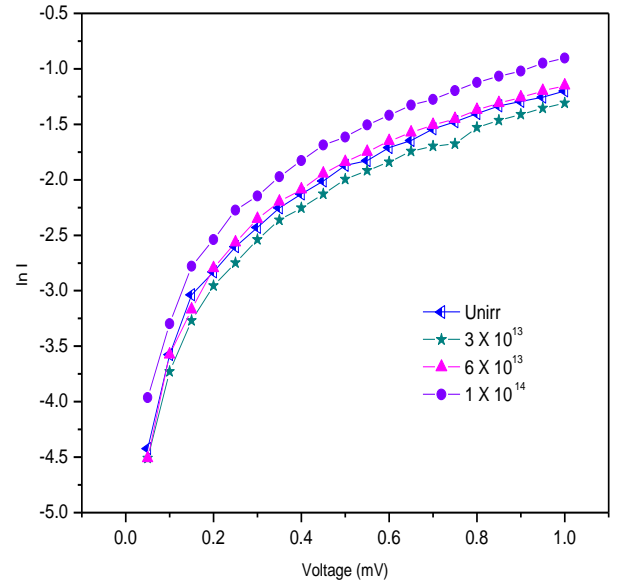


Figure 6: Semi logarithmic I-V characteristics of the as-deposited and irradiated Zr/n-Si samples

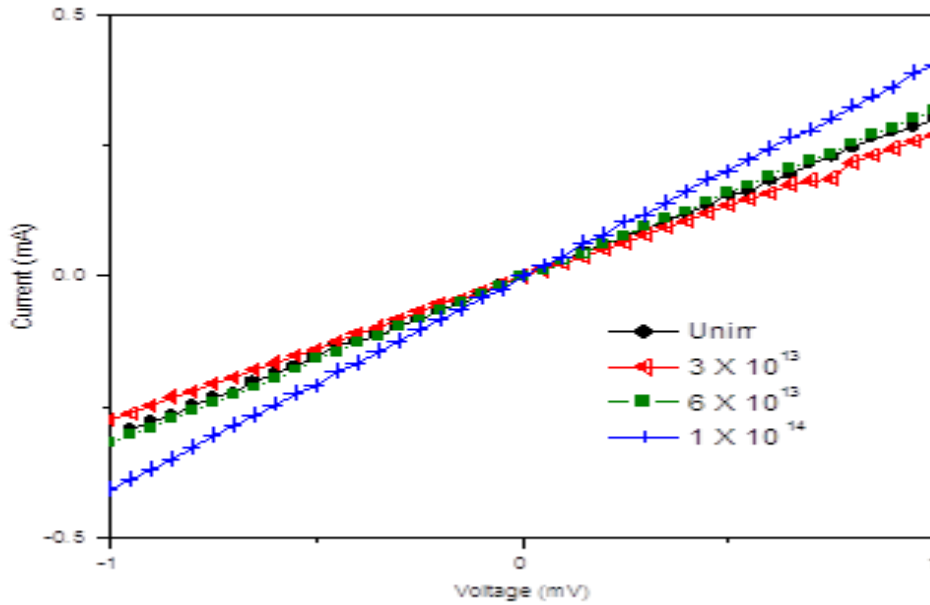


Figure 5: I-V characteristics of the as-deposited and irradiated Zr/n-Si samples showing the formation of Ohmic contact.

(FWHM), strain (ϵ) and the dislocation density (δ) is also evaluated.

From the calculated microstructural parameters in Table 1, it is clear that the crystallite size of $ZrSi_2$ decreases with an increase in ion fluency while the dislocation density increases. This may be attributed to a sudden increase in temperature at the irradiation regime or it may be due to the lattice mismatch between Zr silicide and Si substrate. It could have been the fact that *SHI* irradiation induced electronic excitation along with thermal spikes may cause atomic redistribution and diffusion of Zr and Si at the interface of Zr/Si thin films, due to which $ZrSi_2$ formation has taken place sequentially.

The surface Morphologie

SEM and AFM measurements

The SEM images obtained from Zr–Si thin film system irradiated by 150 MeV Au ions at RT are shown in figure 2 for doses of 3×10^{13} – 1×10^{14} ions/cm². It is clearly evident from the figure that Zr–Si silicide films irradiated by Au ions exhibit considerably different polycrystalline film morphology with film thickness, viz., non-uniform, relatively large grains, accompanying with high roughness, high Si concentration and lattice defects.

Pattern obtained from the unirradiated samples exhibit a complex polycrystalline structure, consisting of large grains with well-defined grain boundaries of relatively small voided regions of exposed Si. In the case of the Zr–Si silicide film irradiated with 3×10^{13} these large grains with existence of $ZrSi_2$ are separated from one another by well-defined grain boundaries, with relatively large voided regions. These grain boundaries are characterized by holes.

For the samples irradiated with 6×10^{13} and 1×10^{14} ions/cm², these holes seem to coalesce into larger ones and finally some holes on the grain boundaries even grow in size until a visible (or continuous) hole exists from the top of the Si-rich silicide

islands to the silicon substrate. In addition Si-enriched silicide islands with visible hole seem to precipitate finely in Si matrix. In other words, for the films irradiated with 6×10^{13} , $ZrSi_2$ agglomeration is accompanied with grain boundary grooving, followed by grain separation and formation of Si-rich silicide islands.

Corresponding to this sample, our XRD analysis yields an average grain size, $D = 69.0$ nm for the film (Table 1) and an average grain size values of 73.5, 67.7 and 74.69 nm for $ZrSi_2(111)$, $ZrSi_2(152)$ and $ZrSi_2(2\ 42)$ phases.

Our SEM measurements also show that as the irradiation dose increases from 3×10^{13} – 1×10^{14} ions/cm², the $ZrSi_2$ surface grains existing in silicon matrix start to agglomerate and become larger in size. Where XRD analysis yields an average grain sizes 67.14, 67.54 and 67.45 nm for $ZrSi_2(111)$, (242) and (152) planes, respectively, while the voided regions of exposed Si (or holes) become larger.

To examine the surface morphology of these samples, atomic force microscopy measurements were carried in non contact mode for different irradiation doses using a Multimode Scanning Probe Microscope (Zeol-JPSM 5200) machine in university of Pune. Figure 3 shows the AFM images for different irradiation doses. At lower fluence, pillar-like structures of average height 32 nm are observed. After more doses a reduce in average height is observed to 25 nm. As the irradiation dose is increased these pillar-like structures transforms to a more hill type structure as also observed in Ti/Si system by S. Ilango and co-workers (2005).

Based on the AFM analysis, shown in figure 3b and d, as the irradiation dose increases from 3×10^{13} to 1×10^{14} , the average grain diameter of the Zr–Si films increases from 23 to 80 nm. The mean roughness values corresponding to the film agglomeration also increases 23–50 nm (about 2 times) due

to the phase transformation from the Zr-rich silicide phases to the Si-rich silicide phases. Thus AFM studies of Au irradiated Zr/Si thin film system shows a trend of increasing average diameter and mean roughness values, with increasing irradiation doses.

Electrical transport studies

The electrical resistivity of the Zr–Si silicide films irradiated at different doses has been measured for the room temperature (at 295 K).

Figure 4 shows the variation of resistivity of the Zr–Si silicide films as function of the Au ion doses. It is clearly seen from the figure that there is a significant decrease in the resistivity of the Zr–Si silicide films with increasing ion doses. These results clearly indicate that the resistivity of the Zr/Si samples is significantly dependent on the silicide film thickness via incident ion doses. The reason might be that by the irradiation, structural relaxation and annealing processes are generated in the films. Also, irradiation leads to a widening of the open channels and a constriction of the conducting paths. Thus there are two simultaneously acting phenomenon (i) change in resistance due to changes in the film topography, (ii) change in resistance due to relaxation and annealing process. In our case a resistance decreases for the increasing fluences the resistance decrease mechanism is dominant leading to the observed decrease of the resistivity.

I–V (current–voltage) data of electronic transport across the bilayer of the Zr/n-Si interface has been recorded both for the irradiated and un-irradiated ones, shown in figure 5. The current across the interface was measured from the top and bottom electrical contacts across the bilayer structure using a Keithley 2400 source measure unit.

Furthermore, the barrier height (ϕ_b) and the ideality factor (n) of the Schottky diodes were derived from the current function of forward biased voltage using thermionic emission model as follows:

$$I = AA^*T^2 \exp (q\phi_b / kT) (\exp \{-qV_{eff}/nkT\} - 1) \dots (A)$$

where A^* is the Richardson constant ($A^* = [(4\pi m^* k^2 e) / h^3] = 31.2 \text{ A/cm}^2 \text{K}^2$ for n-Si), T the temperature in Kelvins, k the Boltzmann constant, q electronic charge, V_{eff} the effective bias across the interface, n the ideality factor, m^* effective mass of the conduction electrons in Si ($= 0.26m_0$), h Planck’s constant and m_0 the rest mass of electron. We resolved (A) for a straight line equation, in a way to plot $\log I_0$ on the y-axis and applied bias on the x-axis to obtain the intercept at y-axis in terms of saturation current, from the semilogarithmic I–V curve shown in Fig.6 . From equation (A) the calculated saturation current I_s is:

$$I_s = AA^*T^2 \exp (q\phi_b / kT) \dots (B)$$

Thus the barrier height is

$$\phi_b = kT/q \ln (AA^*T^2 / I_s) \dots (C)$$

The Schottky barrier height of Zr/n-Si were deduced with expressions (A) and (B) above and they are displayed in Table 2. It is seen that the range for the barrier height of the diodes was from 0.62 eV to 0.58 eV, here the ideality factor was close to 1.

Conclusion

Zr/n-Si bilayer structures have been fabricated and irradiated by 150 MeV Au⁹⁺ ions with a fluence of 3×10^{13} - 1×10^{14} ions/cm². Silicide formation in Zr/Si system has been investigated using XRD, SEM and AFM techniques. The silicide formation starts at the lowest fluence, 3×10^{13} ions/cm², of incident Au ions with the Zr over-layer gradually getting converted to crystalline phases of ZrSi₂. On characterization from AFM and XRD, the formation of granular silicide phase of silicon rich silicide ZrSi₂ has been found. XRD results show that well-crystallized C-49 ZrSi₂ phase was formed in the last two samples. Besides, with increasing ion dose, the electronic transport data show that the resistivity decreased and

dropped sharply to a value of $84\mu\Omega\cdot\text{cm}$ at a dose of 3×10^{13} ions/ cm^2 , and that further decreased, down to $36\mu\Omega\cdot\text{cm}$ at a dose of 1×10^{14} ions/ cm^2 . Atomic force microscopy has revealed noticeable surface changes upon swift heavy ion irradiation. A comparison of the experimental results is presented elucidating the irradiation effects in Zr/Si thin film system. I-V characteristics and Schottky barrier height calculation show a significant effect of irradiation on bilayer structure of Zr/n-Si. The barrier height of the silicide decreases with the increasing ion dose and the results are well in accordance with the barrier formation models that are based on Fermi-level pinning in the centre of the indirect band gap.

References

- [1]. W. Xia, C. A. Hewett, M. Fernandes, S. S. Lau, and D. B. Poker, *J. Appl. Phys.* 65 (1989) pp 2300-2305.
- [2]. A. H. Hamdi and M.-A. Nicolet, *Thin Solid Films* 119 (1984) pp 357-361.
- [3]. L. Niewoñner and D. Depta, *Nucl. Instrum. Methods Phys. Res. B* 59 (1991) pp 523-527.
- [4]. M. Ye, E. P. Burte, and H. Ryssel, *Nucl. Instrum. Methods Phys. Res. B* 59 (1991) pp 528-531
- [5]. C. Dehm, I. Kasko, E. P. Burte, J. Gyulai, and H. Ryssel, *Appl. Surf. Sci.* 73 (1993) pp 268-272
- [6]. I. Kasko, C. Dehm, L. Frey, and H. Ryssel, *Nucl. Instrum. Methods Phys. Res. B* 81 (1993) pp 786-791
- [7]. A. Baba, H. Aramaki, T. Sadoh, and T. Tsurushima, *J. Appl. Phys.* 82 (1997) pp 5480-5484
- [8]. S. Kal, I. Kasko, and H. Ryssel, *J. Electron. Mater.* 24 (1995) pp 1349-1352
- [9]. L. S. Hung, Q. Z. Hong, and J. W. Mayer, *Nucl. Instrum. Methods Phys. Res. B* 37 (1989) pp 414-419
- [10]. L. S. Wielunski, C-D. Lien, B-X Liu and M-A. Nicolet, *Metastable Materials Formation by Ion Implantation*, North-Holland, New York (1982) pp 139-145
- [11]. S.P. Murarka, *J. Vac. Sci. Technol.* 17 (1980) pp 775-779
- [12]. S.P. Murarka and D B Fraser, *J. Appl. Phys.* 51 (1980) pp 350-355
- [13]. F.M. d'Heurle, *J. Mater. Res.* 3 (1998) pp 167-173
- [14]. H. Jeon, C.A. Sukow, J.W. Honecutt, G.A. Rozgonyi, R.J. Nemanich, *J. Appl. Phys.* 71 (1992) pp 4269-4273
- [15]. K. Maex, *Mater. Sci. Eng.* R11 (1992) pp 53-57
- [16]. C. A. Sukow, R. J. Nemanich, *J. Mater. Res.* 9 (1994) pp 1214-1219
- [17]. H. Jeon, S. Kim, *Japan. J. Appl. Phys.* 37 (1998) pp 4747-4752
- [18]. S.S. Lau, W.K. Chu, J.W. Mayer, K. N. Tu, *Thin Solid Films* 23 (1974) pp 205-209
- [19]. M. Setton, J. Van der Spiegel, *J. Appl. Phys.* 70 (1991) pp 193-197
- [20]. J.H. Lin, W.Y. Hsieh, L.J. Chen, *J. Appl. Phys.* 79 (1996) pp 9123-9127
- [21]. A. Bourret, F.M. d'Heurle, F. K. Le Goues, A. Charai, *J. Appl. Phys.* 67 (1990) pp 241-246
- [22]. X. Zhao, D. Ceresoli, D. Vanderbilt, *Phys. Rev. B* 71 (2005) pp 85107-85112
- [23]. J.F. Zeigler, J.P. Biersack, U. Littmark, *The Stopping Range of Ions in Solids*, Pergamon Press, New York (1985).
- [24]. S. Ilango, G. Raghavan, M. Kamruddin, S. Bera, A.K. Tyagi, *Appl. Phys. Lett.* 87 (2005) pp 101911-101918.